

# Complex Valued Sphere Decoding with Element-wise Selective Prescreening for General Two-dimensional Signal Constellations

Hwanchol Jang, Saeid Nooshabadi, *Senior Member, IEEE*, Kiseon Kim, *Senior Member, IEEE*, and  
Heung-No Lee\*, *Senior Member, IEEE*

**Abstract**—Sphere decoding (SD) is a promising detection strategy for multiple-input multiple-output (MIMO) systems because it can achieve maximum-likelihood (ML) detection performance with reasonable complexity. The standard and most SD algorithms operate on real valued systems. These real valued SDs (RV-SDs) are known to be applicable to MIMO communication systems with only rectangular QAM signal constellations. In addition to this restriction on applicable constellations, RV-SDs are not suitable for VLSI implementations. Complex valued SD (CV-SD) is a good SD candidate for its flexibility on the choice of constellations and its efficiency in VLSI implementations. But, the low complexity CV-SD algorithm for general two dimensional (2D) constellations is not available, especially with the one that attains the ML performance. In this paper, we present a low complexity CV-SD algorithm, referred to as Circular Sphere Decoding (CSD) which is applicable to arbitrary 2D constellations. CSD provides a new constraint test. This constraint test is carefully designed so that the element-wise dependency is removed in the metric computation of the test. As a result, the constraint test becomes simple to perform without restriction on its constellation structure. By additionally employing this simple test as a prescreening test, CSD reduces the complexity of the CV-SD search. Through the analysis and simulations, we show that the complexity reduction is significant while its ML performance is not compromised.

**Index Terms**—multiple input multiple output (MIMO), circular sphere decoding (CSD), sphere decoding (SD), complex valued, complex valued sphere decoding, arbitrary constellation

## I. INTRODUCTION

**S**PHERE decoding (SD) is a promising multiple-input multiple-output (MIMO) detection strategy because it can achieve the error rate of maximum-likelihood (ML) detector with significantly less complexity compared to the straight-forward ML detector [1]-[4]. The standard and most SDs are real valued SDs (RV-SDs) which are only directly

applicable to real valued systems. For the usages of RV-SDs, the complex valued system is decomposed into its real and imaginary parts, and it becomes a real valued equivalent system with twice the dimension of its complex valued counterpart. Here note that SD assumes each substream of data modulated independently. This independency is kept for its real valued equivalent system model when each substream is modulated by rectangular QAMs. Pham et al. [5] and Mozos and Garcia [6] stated that the application of RV-SD is permissible only for rectangular QAMs because otherwise invalid candidates may arise during the search; it is because the independency between the substream is broken.

It is desirable for an SD to be applicable directly on complex valued systems in the senses of *i*) its flexibility on the choice of signal constellations and *ii*) its efficiency in VLSI implementations. *i*): Complex valued SDs (CV-SDs), which are applicable directly on complex valued systems, do not require the decomposition of the systems, and the limitation of rectangular QAM can be eliminated. Each substream of data can be modulated using any two dimensional (2D) constellations. There are many constellations which are desirable to be employed in terms of many aspects of communications performance over rectangular QAMs. The benefits include the reduction in peak-to-average power ratio (PAPR) at each transmit antenna, SNR efficiency, and the increased range of choice for its data rate. To list a couple of examples, star QAM reduces the PAPR [7], and near-Gaussian constellations give the shaping gain [8], [9]; rectangular QAMs depart significantly from these constellations. *ii*): Burg et al. show that the expected number of nodes visited in the SD search is nearly doubled when a complex valued system is decomposed into its equivalent real valued system and RV-SD is used [10]. Although the processing for each visit of a node becomes simpler in RV-SD, the processing is not simple enough to compensate the increase in the number of visits. They conclude that CV-SD is essential to achieve high throughput VLSI implementations [10], [11].

In CV-SDs, however, the main operation of SD, the pruning test is complex. The test relies on partial Euclidean distance (PED) computations. Here, PED computations are complex, actually the most cost expensive operations in SD, and thus, the CV-SD has high complexity. In previous CV-SDs, it is considered to restrict the applicable constellation only to those

Hwanchol Jang, Kiseon Kim and Heung-No Lee are with the Department of Information and Communications, Gwangju Institute of Science and Technology, Gwangju, 500-712 Korea, e-mail: {hcjang, kskim, heungno}@gist.ac.kr. The asterisk \* indicates the corresponding author.

Saeid Nooshabadi is with the Department of Electrical and Computer Engineering and the Department of Computer Science, the Michigan Technological University, Houghton, MI, 49931, e-mail:saeid@mtu.edu.

whose elements are aligned in concentric rings with different radii for complexity reduction [5], [10]-[12]. Hochwald and Brink propose to use an interval for phases of constellation points, rather than complex value itself, for the pruning test [12]. Pham et al. apply the Schnorr-Euchner enumeration on the interval [5]. Burg et al. improve it by additional complexity reduction on the enumeration [10], [11]. Nevertheless, the general CV-SD without restriction on its constellation is still remained to be complex.

It is our goal in this paper, therefore, to develop a low complexity CV-SD for general 2D constellations. We aim to do this while guaranteeing the ML performance. To this end, we take a new approach which takes advantage of a simple necessary condition, rather than an equivalent one, of the original pruning constraint, the sphere constraint (SC). We generate the necessary condition such that the metric for the constraint test becomes the magnitude of a scalar, not the Euclidean distance of a vector, thus the constraint test becomes very simple. We propose to use the necessary condition as a prescreening test, and use it for complexity reduction for the CV-SD. The proposed constraint and the proposed CV-SD algorithm employing the constraint are referred to as the circular constraint (CC) and circular sphere decoding (CSD), respectively. CSD employs a two-step constraint test. In the prescreening step, those constellation points which are not promising are eliminated by the simple CC tests. The pruning by SC tests, in the second step, requiring expensive PED calculations is performed only for those candidates which are composed of the surviving constellation points in the CC tests. Thus, many complex PED computations are avoided. Significant savings in the complexity of the CV-SD can be made, we show in theoretical analysis and also in simulation, with CSD without sacrificing the ML performance.

The rest of this paper is organized as follows. In Section II, the system model is presented. In Section III, the underlying principle in SD, and the difference between RV-SD and CV-SD are studied. In Section IV, the proposed CSD algorithm is developed. In Section V, the complexity analysis for the CV-SD and the proposed CSD is given. In Section VI, we discuss the system simulation results. Section VII concludes the paper.

## II. SYSTEM MODEL AND NOTATION

We consider a complex-valued baseband MIMO channel model with  $m$  receive and  $n$  transmit antennas ( $m \geq n$ ). Consider the system model,

$$\mathbf{r} = \mathbf{H}\bar{\mathbf{s}} + \mathbf{v}, \quad (1)$$

where  $\mathbf{r} \in \mathbb{C}^m$  denotes the received signal,  $\mathbf{H} \in \mathbb{C}^{m \times n}$  denotes the  $m \times n$  block Rayleigh fading channel matrix whose entries are independently and identically distributed (i.i.d.) circularly-symmetric complex Gaussian (CSCG) random variables  $\mathcal{CN}(0,1)$ ,  $\bar{\mathbf{s}} \in \mathcal{O}^n \subset \mathbb{C}^n$  is the transmitted symbol vector where  $\mathcal{O} := \{o_1, o_2, \dots, o_L\}$  can be any discrete 2D constellation set with size  $L$ ;  $o_i \in \mathbb{C}$  for  $1 \leq i \leq L$ . The

components of  $\bar{\mathbf{s}}$  are i.i.d. and take the values uniformly from  $\mathcal{O}$ ,  $\bar{s}_k \in \mathcal{O}$ , and they are scaled to have  $E|\bar{s}_k|^2 = 1$  for  $\forall 1 \leq k \leq n$ . The  $m \times 1$  vector  $\mathbf{v} \in \mathbb{C}^m$  is the additive noise whose entries are i.i.d. CSCG random variables  $\mathcal{CN}(0, \sigma_v^2)$ . The channel  $\mathbf{H}$  is assumed to be known at the receiver.

Variables that denote vectors and matrices are set, respectively, lowercase and uppercase boldface.  $\mathbf{H}_{k,-}$  and  $\mathbf{H}_{-,j}$  denotes the  $k^{\text{th}}$  row and the  $j^{\text{th}}$  column of matrix  $\mathbf{H}$ , respectively.  $\mathbf{H}^*$  and  $\mathbf{H}^\dagger$  denote the conjugate transpose and the pseudo-inverse of  $\mathbf{H}$ , respectively. Each component of a matrix or a vector is denoted by the subscript. For example,  $H_{i,j}$  and  $s_k$  are the  $(i,j)$  component of  $\mathbf{H}$  and, the  $k^{\text{th}}$  component of  $\mathbf{s}$ , respectively.  $\mathbf{s}_{k:n}$  is the vector taking the last  $n - k + 1$  components of  $\mathbf{s}$ .  $|\mathcal{O}|$  denotes the cardinality of the set  $\mathcal{O}$ .  $|a|$  denotes the magnitude of  $a \in \mathbb{C}$ .  $\|\mathbf{s}\|$  denotes the  $2^{\text{nd}}$  norm of vector  $\mathbf{s}$ .  $\mathbb{R}$  and  $\mathbb{C}$  denote the real and the complex domains respectively.  $\Re(s_k)$  and  $\Im(s_k)$  denote the real and the imaginary parts of  $s_k$  respectively.

## III. STUDY ON SPHERE DECODING PRINCIPLE

In this section, we describe the SD principle and the complexity problem in CV-SD.

### A. SD principle

The standard procedure of SD is *i*) to identify all the candidates  $\mathbf{s}$  which satisfy the sphere constraint (SC), and *ii*) to choose the candidate with the minimum distance to the received signal  $\mathbf{r}$  as the solution. The SC is expressed by

$$d(\mathbf{s}) := \|\mathbf{r} - \mathbf{H}\mathbf{s}\|^2 = \sum_{k=1}^n |e_{\mathbf{H},k}(\mathbf{s})|^2 \leq C, \quad (2)$$

where  $\mathbf{s} \in \mathcal{O}^n$  and  $e_{\mathbf{H},k}(\mathbf{s}) = r_k - \mathbf{H}_{k,-}\mathbf{s}$ . The SC test may be done by computing  $d(\mathbf{s})$  for all  $\mathbf{s}$  and comparing it with  $C$ . But, the expression for Euclidean distance (ED)  $d(\mathbf{s}) := \|\mathbf{r} - \mathbf{H}\mathbf{s}\|^2$  is not a desirable form for calculation. It is because  $e_{\mathbf{H},k}(\mathbf{s})$  is a function of whole elements of  $\mathbf{s}$ . For example, even two slightly different candidates, say, of which only a single element value of  $\mathbf{s}$  is different, require two separate ED calculations, two computations of  $|e_{\mathbf{H},k}(\mathbf{s})|^2$ , for each level  $1 \leq k \leq n$ . The SC can be written also as

$$d_i(\mathbf{s}_{i:n}) := \|\mathbf{R}_{i:n,-}(\mathbf{x} - \mathbf{s})\|^2 = \sum_{k=i}^n |e_{\mathbf{R},k}(\mathbf{s}_{k:n})|^2 \leq C, \text{ for } 1 \leq i \leq n, \quad (3)$$

with  $\mathbf{R}$  the upper triangular matrix from the QR decomposition of  $\mathbf{H}$ ,  $e_{\mathbf{R},k}(\mathbf{s}_{k:n}) = \mathbf{R}_{k,k:n}(\mathbf{x}_{k:n} - \mathbf{s}_{k:n})$  and  $\mathbf{x} := \mathbf{H}^\dagger \mathbf{r}$  where  $\mathbf{H}^\dagger := (\mathbf{H}^* \mathbf{H})^{-1} \mathbf{H}^*$ . Assume that the value of  $s_l$  for any  $1 \leq l \leq n$  changes. The distance calculation of the  $k^{\text{th}}$  level of the tree,  $|e_{\mathbf{R},k}(\mathbf{s}_{k:n})|^2$ , for level  $k > l$  do not need to be done again. It

now becomes partially dependent, hence gives computational savings to SD. Here,  $d_k(\mathbf{s}_{k:n})$  is referred to as partial Euclidean distance (PED) and it depends only on the partial vector  $\mathbf{s}_{k:n}$ , the last  $n-k+1$  components of  $\mathbf{s}$ , which is associated with the nodes at the  $k^{\text{th}}$  level of the tree. As PED is monotonically increasing as  $k$  decreases, PEDs for the remaining levels of  $k$  do not need to be computed once PED of a level is found to violate the SC in (3). This gives additional computational savings. As a result, the SC in (3) is used in actual SDs and gives complexity reductions.

Here, we should note that PED computation is still complex, actually the most complex operation in SD, as there is still the dependency on the elements of  $\mathbf{s}$  in distance calculations. For a lower complexity algorithm, it is helpful to reduce the number of explicit PED computations in SD. This can be done in a way by employing a simplified SC where explicit PED computations are not required, rather than the SC in (3). In the past, further simplification on SC is obtained, as noted in the introduction, by employing rectangular QAMs and exploiting the characteristics that exists in the constellations.

### B. The difference between RV-SD and CV-SD

The SC in (3) can be written as follows by a few manipulations

$$\left| \frac{b_i}{R_{i,i}} - s_i \right|^2 \leq \frac{C - d_{i+1}(\mathbf{s}_{i+1:n})}{R_{i,i}^2}, \quad i = 1, 2, \dots, n-1 \quad (4)$$

where  $b_i := \mathbf{R}_{i,i:n} \mathbf{x}_{i:n} - \mathbf{R}_{i,i+1:n} \mathbf{s}_{i+1:n}$ . In real valued systems where the components of  $\mathbf{r}$ ,  $\mathbf{H}$ ,  $\bar{\mathbf{s}}$ ,  $\mathbf{s}$ , and  $\mathbf{v}$  are real valued, (4) can be simplified by the so called admissible interval (AI) which is expressed by the lower limit  $s_i^l$  and the upper limit  $s_i^u$  as follows

$$s_i \in [s_i^l, s_i^u], \quad (5)$$

where  $s_i^l = \frac{b_i}{R_{i,i}} - \frac{\sqrt{C - d_{i+1}(\mathbf{s}_{i+1:n})}}{R_{i,i}}$  and  $s_i^u = \frac{b_i}{R_{i,i}} + \frac{\sqrt{C - d_{i+1}(\mathbf{s}_{i+1:n})}}{R_{i,i}}$ . The AI in (5) is a SC which is equivalent to (3) and (4) for real valued systems. Here note that it is simpler to compute than (3) or (4) and it is used in RV-SD instead of the SC of (3). The AI is still element-wise dependent since  $b_i$  and  $d_{i+1}(\mathbf{s}_{i+1:n})$  are functions of  $\mathbf{s}_{i+1:n}$ . But it can be identified by calculating only the two values,  $s_i^l$  and  $s_i^u$ . The constellation points  $s_i$  which satisfy the SC (2) can now be identified using (5) without PED computations  $d_i(\mathbf{s}_{i:n})$  of whole candidates  $\mathbf{s}_{i:n}$  for the current level  $i$  of the tree. Here note that PED computations are still needed in the RV-SD. They are not for pruning itself but for setting the AI,  $s_{i-1}^l$  and  $s_{i-1}^u$ , for the next level of the tree; the computations of  $d_i(\mathbf{s}_{i:n})$ . This requires PED computations but only for the nodes in the AI. Therefore, the number of PED computations is reduced in the RV-SD. However, please note that, this SD by AI (5) applies only to rectangular QAMs. Refer to [2]-[4] for more conceptual description of RV-SD.

In this work, the aim is for a CV-SD for general 2D constellations. This makes it difficult to replace the complex operations for the SC in (3) with cheaper operations. Hence, every single pruning in the CV-SD is done by the explicit complex PED computations for the SC test (3) [10], [11]. This results in high complexity in the CV-SD; the discussion on the complexity comparison to the RV-SD is given in Section V.

Let us see the difference on the number of PED computations of the CV-SD and the RV-SD. Consider a tree which is used for the SD search. The tree expands with the factor  $L$  as the level of the tree,  $k$ , goes down, starting from  $k = n$  to  $k = 1$ . The number of nodes at the  $k^{\text{th}}$  level of the tree is  $L^{n-k+1}$  and each node represents a candidate for the partial vector  $\mathbf{s}_{k:n}$ . Assume that there are  $N_{k+1}^{\text{sc}}$  nodes which satisfy the SC at  $(k+1)^{\text{th}}$  level of the tree. In the CV-SD, all the children nodes of the surviving nodes are calculated for their PEDs. That is  $L \cdot N_{k+1}^{\text{sc}}$  PED computations for the  $k^{\text{th}}$  level of the tree. We name this *L-expansion property* of the CV-SD. This is trivial but it will be easier for us to recall this property later on. In the RV-SD, only the  $N_k^{\text{sc}}$  nodes which are inside the AI at the  $k^{\text{th}}$  level of the tree are required for PED computations for the level of the tree. Surely,  $L \cdot N_{k+1}^{\text{sc}} \geq N_k^{\text{sc}}$ . The gap between these two is analyzed further in Section V.

Hochwald and Brink [12], Burg et al. [10], [11], Pham et al. [5], and Mozos and Garcia [6] consider restricting the applicable signal constellations only to those whose elements are aligned in several concentric rings with different sizes, rather than general 2D constellations, so that they can exploit the constellation structure. An AI is obtained for these complex valued constellations. There, the interval is not for the value of  $s_k$  itself but for its phase  $\angle s_k$ , hence computation of it requires trigonometric operations. In this paper, we do not consider this approach. Obviously the applicability of the method is limited to only those constellations with specific shapes. In addition, it requires costly trigonometric function and other computations. Note also that the one in [13] considers a fixed complexity realization of CV-SD. It reduces the complexity for general CV-SD. But we also do not consider this in this paper since it sacrifices the ML performance for its complexity.

## IV. PROPOSED CIRCULAR SPHERE DECODING

The applicability to general 2D constellations is an important benefit of the CV-SD. But, this benefit gives an inherent problem in the CV-SD. No structure of a specific constellation can be exploited for a simplification of the SC in (3) because it needs to work for general 2D constellations. This makes it difficult to have a simpler but equivalent constraint to the SC. Hence, the CV-SD relies on costly PED based SC tests for pruning.

In this section, we simplify the complex SC by resorting to one of its necessary conditions, rather than to any specific structure in constellations. We refer to the necessary condition as the circular constraint (CC). Since the CC is a necessary condition,

it may not prune as tightly as the SC may. Not to lose any pruning efficiency in the CV-SD, SC tests are executed for those nodes which are not eliminated by the preceded CC tests. We call this CV-SD employing CC circular sphere decoding (CSD). CSD prunes the nodes the same amount as the baseline CV-SD does but with a much smaller number of explicit PED computations. Here, CSD is efficient, since the overhead for employing CC is negligible. The cost for CC tests is very small because CC is derived so that the element-wise dependency is removed inside the norm calculation in (3).

#### A. Circular constraint (CC)

PED is still complex as there is dependency on the elements of  $\mathbf{s}$  in the computation (3); the change of the value for, say,  $s_l$  ( $1 \leq l \leq n$ ) changes the distance calculation of the  $k^{\text{th}}$  level of the tree  $|e_{\mathbf{r},k}(s_{k:n})|$  not only for level  $k = l$  but also for level  $1 \leq k < l$ . Now, we aim to find a metric with which the SC can be simplified so that the element-wise dependency is removed. We start from the SC in (2). The element-wise dependency is removed by eliminating the channel matrix  $\mathbf{H}$  inside the norm operator. The derivation is given by

$$\begin{aligned}
 C &\geq \|\mathbf{H}(\mathbf{x}-\mathbf{s})\|^2 \\
 &= \frac{\|\mathbf{H}^\dagger_{k,-}\|^2}{\|\mathbf{H}^\dagger_{k,-}\|^2} \|\mathbf{H}(\mathbf{x}-\mathbf{s})\|^2 \\
 &= \frac{\|\mathbf{H}^\dagger_{k,-}\|^2}{\|\mathbf{H}^\dagger_{k,-}\|^2} \|\mathbf{H}(\mathbf{x}-\mathbf{s})^*\|^2 \\
 &\stackrel{(a)}{\geq} \frac{|\mathbf{H}^\dagger_{k,-} \mathbf{H}(\mathbf{x}-\mathbf{s})|^2}{\|\mathbf{H}^\dagger_{k,-}\|^2} \\
 &\stackrel{(b)}{=} \frac{|x_k - s_k|^2}{\|\mathbf{H}^\dagger_{k,-}\|^2},
 \end{aligned} \tag{6}$$

where (a) is from the Cauchy-Schwarz inequality and (b) is from the fact that  $\mathbf{H}^\dagger \mathbf{H}(\mathbf{x}-\mathbf{s}) = \mathbf{x}-\mathbf{s}$  with the assumption that  $\mathbf{H} \in \mathbb{C}^{m \times n}$  has the full rank with  $m \geq n$ . For a  $\mathbf{H}$  with rank deficiency, there are contributions in the metric derived in (6) from the elements of  $\mathbf{x}-\mathbf{s}$  other than the  $k^{\text{th}}$  element of it. But, they are insignificant unless  $\mathbf{H}$  has serious rank deficiency.

Now, we have new constraint, CC,

$$\Delta_k(s_k) \leq C \cdot \delta_k^2, \quad k = 1, 2, \dots, n, \tag{7}$$

where  $\Delta_k(s_k) := |x_k - s_k|^2$  and  $\delta_k^2 := \|\mathbf{H}^\dagger_{k,-}\|^2$ . We name the metric  $\Delta_k(s_k)$  in CC as circular metric (C-metric). Here,  $\delta_k^2$  can be computed before the SD search begins and the value of  $\delta_k^2$  does not change until the channel matrix  $\mathbf{H}$  gets changed, thus it can be used while  $\mathbf{H}$  stays the same. Please note that CC is a necessary condition for a candidate  $\mathbf{s}$  to satisfy the SC in (2). It is because the metric derived in (6) is smaller than or equal to the Euclidean metric for original SC in (2).

*Definition 1: (element-wise independent metric)* We call a metric is *element-wise independent* if the metric at a level of tree, say the  $k^{\text{th}}$  level, depends only on the value of the corresponding element  $s_k$ , but not on that of any  $s_l$  where  $l \in \{1, 2, \dots, n\}$  and  $l \neq k$ . Note that this element-wise independence is different from the statistical independence between two random variables.

The C-metric  $\Delta_k(s_k)$  is element-wise independent since  $\Delta_k(s_k)$  depends only on  $s_k$ . This element-wise independence gives CC two beneficial features. First, the number of C-metric computations required for CC tests is fixed only to  $L$  for each level of the tree. There are  $L^{n-k+1}$  number of nodes at the  $k^{\text{th}}$  level of the tree. This many PED computations may be required for SC tests in the CV-SD. But, the number of C-metric computations for any level of the tree is fixed only to  $L$ , rather than  $L^{n-k+1}$ , it is because a C-metric does not depend on the elements of the parent node, *i.e.* element-wise independent, and hence the C-metrics for the children nodes generated from one parent node are the same with those from another parent node. Second, C-metric computation is simple. A C-metric computation requires only five floating point operations (FLOPs), very simple compared to a PED computation; a PED computation requires  $10(n-k)+8$  FLOPs.<sup>1</sup> Here also note that the actual cost for a C-metric computation when the CC test is followed by a SC test is only three FLOPs. It is because a PED computation follows in this case, and a part of the C-metric computation is reused for the following PED computation.

Thanks to these two benefits, the complexity for CC tests is negligible compared to that of SC tests.

#### B. Circular sphere decoding

In CSD, we utilize the simple CC for prescreening on the SC tests which require expensive PED computations, thus reduce the number of PED computations in the search. The strategy in CSD is *i)* to eliminate nodes as many as possible for a given level of the tree using the CC, and then *ii)* to perform PED computations only for the surviving nodes for the SC test in (3).

Consider Fig. 1 where we specify the CSD operations by providing the geometry of the CC and the SC. The CC is represented in the  $\mathbf{s}$  space by  $n$  separate circles, one for each element of  $\mathbf{s}$ . The SC is represented by the sphere in the  $\mathbf{H}\mathbf{s}$  space. In the prescreening step of CSD, the constellation points which are not inside each separate circle are excluded in the search. In the pruning step, the process of identifying vector points which are inside the sphere is performed. This process requires PED computations since it is to calculate the norm of a vector. But, this complex PED calculation is performed only for the prescreened candidates. In CSD, many not promising

<sup>1</sup> Computation the  $k^{\text{th}}$  component of  $\mathbf{R}(\mathbf{x}-\mathbf{s})$  requires  $n-k+1$  complex subtractions,  $n-k$  complex multiplications and two multiplications and  $n-k$  complex additions, totaling  $10(n-k)+4$  FLOPs (one complex multiplication and one complex addition are equivalent to six FLOPs and two FLOPs, respectively). Computation of  $|\mathbf{R}(\mathbf{x}-\mathbf{s})|$  requires two multiplications and one addition. Formation of accumulative PED requires another addition.

candidates are eliminated in the prescreening test even before their PEDs are computed. As it is shown in Fig. 1, only a portion of the points are pruned by the SC tests in CSD (Fig. 1 (b)), while whole pruning operations in the CV-SD are through the complex SC test. Thus, the employment of the CC test in CSD reduces the complexity of the CV-SD. As a result, CSD outperforms the CV-SD in terms of complexity (Section V). Note that the ML performance in CSD is not compromised since the CC test does not eliminate the ML solution; the CC is

necessary for the satisfaction of the SC for a candidate.

Note that the proposed CSD can employ statistical pruning techniques such as those in [14]-[16] for additional complexity reduction. This can be done just by replacing the  $C$  by one of those proposed in [14]-[16].

The entire algorithm of the proposed CSD is given in Table I. Note that removing Step 0 (the  $C$ -metric computation) and Step 4 (CC test) in the CSD algorithm makes it equal to the baseline CV-SD.

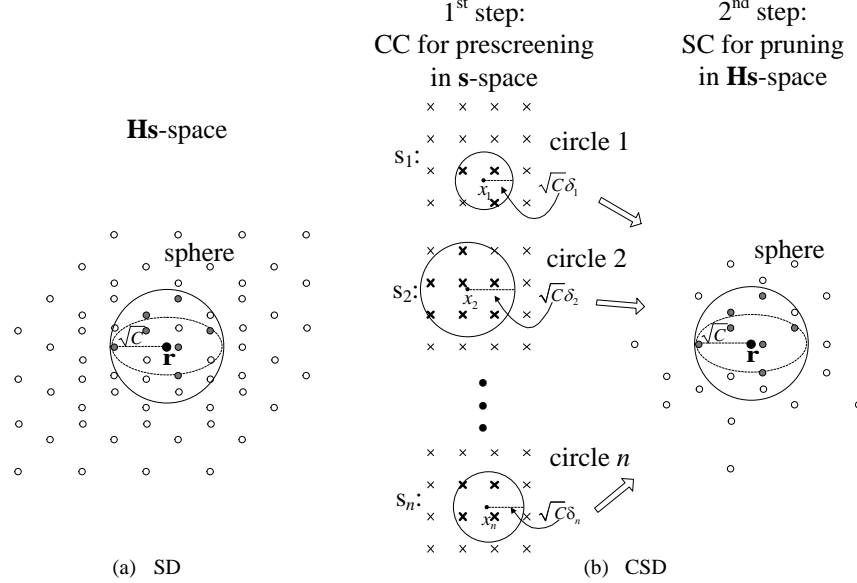


Fig. 1. Geometry of SD and the proposed CSD with 16 QAM constellation (gray-colored points represent those points which are inside the sphere). (a) SD. (b) CSD.

TABLE I

The CSD Algorithm

The CSD Algorithm	
<b>Definitions:</b>	$\mathcal{O} = \{o_1, o_2, \dots, o_L\}$ (the constellation set), $\delta^2 = [\delta_1^2, \delta_2^2, \dots, \delta_n^2]^T$ , $k$ (the current level), $C$ (squared radius), $s = [s_1, s_2, \dots, s_n]^T$ (the currently visited node), $d_k$ (the PED for the current level), $\hat{s}$ (ML solution).
<b>Inputs:</b>	$\mathcal{O}$ , $\delta^2$ , $C_0$ , $r$ , $x$ , and $\mathbf{R}$ .
<b>Outputs:</b>	$\hat{s}$ .
<b>Step 0:</b> (C-metric)	Compute C-metrics $\Delta_k(s_k)$ for $\forall s_k \in \mathcal{O}$ and $\forall k$ .
<b>Step 1:</b> (Initialization)	set $C \leftarrow C_0$ , $k \leftarrow n$ , $found \leftarrow 0$ .
<b>Step 2:</b> (Initialization of the node for a visit)	<b>for</b> $k=1:n$ set $I_k = 1$ and $s_k = o_1$ .
<b>end</b>	Go to step 4
<b>Step 3:</b> (Next node)	<b>if</b> $I_k \neq L$ , set $I_k = I_k + 1$ and $s_k = o_{I_k}$ , and go to step 4 <b>else</b> go to step 8
<b>Step 4:</b> (CC test *)	<b>if</b> $\Delta_k(s_k) \leq C \cdot \delta_k^2$ , go to step 5 <b>else</b> go to step 3
<b>Step 5:</b> (PED)	Compute PED $d_k(s_{k:n})$ .
<b>Step 6:</b> (SC test)	

**if**  $d_k(s_{k:n}) < C$  go to step 7

**else** go to step 3

**Step 7:** (Forward)

**if**  $k=1$ ,  $C \leftarrow d_k$  (radius updates),  $\hat{s} \leftarrow s$ ,  $found \leftarrow 1$ , go to step 3.

**else**  $k \leftarrow k-1$ , go to step 4

**Step 8:** (Backward)

**if**  $k=n$  (root node)

**if**  $found = 0$ ,  $C_0 \leftarrow C_0 + \Delta C_0$  (radius increase), go to step 2

**else** exit

**else**

**for**  $k'=1:k$

set  $I_{k'} = 1$  and  $s_{k'} = o_1$ .

**end**

$k \leftarrow k+1$ , go to step 3

\*  $C \cdot \delta_k^2$  is not computed for every CC test. It is computed only when the radius  $C$  is updated in Step 7.

## V. COMPLEXITY ANALYSIS

In this section, we analyze the expected complexity of the CV-SD and the proposed CSD which are applicable for general 2D constellations. Since no complexity analysis has been provided for CV-SD, no standard complexity measure is

available yet.<sup>2</sup> It is common in RV-SDs to employ the number of nodes visited for the metric for complexity measure [14], [15], [17]-[21].<sup>3</sup> Here, we use the number of PED computations, rather than the number of visited nodes, for the measure of complexity for CV-SD. *i*) it is general as it includes the standard complexity measure of RV-SDs as a special case, and *ii*) it is effective to show the main complexity problem of the CV-SD, the SC test using explicit PED computations even for those nodes which are not to be visited. The point *i*) is true as the number of PED computations in RV-SDs is the same with the number of visited nodes which is a standard measure for complexity in RV-SDs; a PED computation is required for a visit to a node in RV-SDs (Section III).

Here, the objective of the expected complexity analysis is *i*) to understand the behavior of the complexity of the algorithms, and *ii*) to compare the complexity of the two algorithms. We consider a lower bound on the expected complexity so that the final form is simple enough to give clear insight on the behavior of the parameters and on the complexity difference between the two algorithms. In this sense, our analysis is similar to those by Jaldén and Ottersten [19] and Shim and Kang [15]. Vikalo and Hassibi provide the exact expected complexity [17], [18], and Gowaikar and Hassibi provide an upper bound [14]. These approaches are not considered in this paper for their complex expressions as they include integrations; the behavior is hard to interpret in this form. Similar to those of [15], [19]-[21], we do not consider FLOPs for the analysis because *i*) the FLOPs for a PED computation is equal in both algorithms, *ii*) overhead for C-metric computation in CSD is negligible (Section IV), and *iii*) the number of PED computations (or the number of visited nodes in RV-SD cases) directly affects the throughput of the true standard VLSI implementation of SD [10], [11]. By the standard implementation here, we mean the SD architectures that visit a node per cycle; this is reasonable since SD is a sequential search algorithm.

#### A. Overview on the complexities of CV-SD and CSD

Let the number of nodes which satisfy the SC at the  $k^{\text{th}}$  level of the tree be called  $N_k^{\text{sc}}$ , i.e.,

$$N_k^{\text{sc}} := \left| \left\{ \mathbf{s}_{k:n} \in \mathcal{O}^{n-k+1} \mid d_k(\mathbf{s}_{k:n}) \leq C \right\} \right|,$$

where  $d_k(\mathbf{s}_{k:n}) = \sum_{i=k}^n \left| \mathbf{R}_{i,i:n}(\mathbf{x}_{i:n} - \mathbf{s}_{i:n}) \right|^2$   
 $= \sum_{i=k}^n \left| \mathbf{R}_{i,i:n}(\bar{\mathbf{s}}_{i:n} - \mathbf{s}_{i:n}) + \tilde{\mathbf{v}}_i \right|^2$  denotes the PED of  $\mathbf{s}_{k:n}$  and

$\tilde{\mathbf{v}} := \mathbf{Q}^* \mathbf{v}$  whose entries are i.i.d. CSCG random variables, and the number of nodes which satisfy the CC at the  $k^{\text{th}}$  level of the tree be called  $N_k^{\text{cc}}$ ,

<sup>2</sup> Note that the analysis in [17] is not for CV-SD. Even though a complex valued system is considered, RV-SD is applied in [17] via system decomposition.

<sup>3</sup> Those in [14], [17], [18] multiply the FLOPs per node to the number of nodes visited.

$$N_k^{\text{cc}} := \left| \left\{ s_k \in \mathcal{O} \mid \tilde{\Delta}_k(s_k) \leq C \right\} \right|,$$

where  $\tilde{\Delta}_k(s_k) := \delta_k^{-2} |x_k - s_k|^2 = \delta_k^{-2} \left| \bar{s}_k - s_k + \mathbf{R}_{k,-}^\dagger \tilde{\mathbf{v}} \right|^2$  denotes the C-metric of  $s_k$  divided by  $\delta_k^2$  with  $\delta_k^2 = \left\| \mathbf{H}_{k,-}^\dagger \right\|^2 = \left\| \mathbf{R}_{k,-}^\dagger \right\|^2$ . The division is to make the squared circle radius  $C \cdot \delta_k^2$  of the CC to be the same as  $C$ , the squared sphere radius of the SC.

In RV-SD, the complexity is given by

$$\mathcal{C}_{\text{SD-R}} = N_1^{\text{sc}} + N_2^{\text{sc}} + \dots + N_n^{\text{sc}}. \quad (8)$$

Since only those nodes which satisfy the SC at the  $k^{\text{th}}$  level of the tree are required for PED computations, this expression is valid.

In the case of CV-SD, this is not true. The AI is not available in the CV-SD. Recall the  $L$ -expansion property (Section III-B). That is, for the identification of  $N_k^{\text{sc}}$  nodes at the  $k^{\text{th}}$  level of the tree,  $L \cdot N_{k+1}^{\text{sc}}$  PED computations are required; this results in high complexity in the CV-SD. The complexity for the CV-SD is, thus, given by

$$\begin{aligned} \mathcal{C}_{\text{SD-C}} &= L \cdot N_2^{\text{sc}} + \dots + L \cdot N_n^{\text{sc}} + L \cdot N_{n+1}^{\text{sc}} \\ &= \sum_{k=1}^n L \cdot N_{k+1}^{\text{sc}}, \end{aligned} \quad (9)$$

where  $N_{n+1}^{\text{sc}} = 1$ . Here, note that the  $N_k^{\text{sc}}$  in (8) and that in (9) are not identical. Actually, the system model itself for (9) is different from that for (8).

In the case of CSD, the high complexity problem of the CV-SD is alleviated. Among all the possible children nodes of each surviving node at the previous level,  $k+1$ , note that there are  $L$  children nodes, only those children nodes,  $N_k^{\text{cc}} \leq L$  of them, which satisfy the CC are passed for PED computations. The same expansion number  $N_k^{\text{cc}}$  applies to all the surviving nodes of the previous level,  $N_{k+1}^{\text{sc}}$ , because of the element-wise independence of C-metric. The complexity for CSD is given by

$$\begin{aligned} \mathcal{C}_{\text{CSD-C}} &= N_1^{\text{cc}} N_2^{\text{sc}} + \dots + N_{n-1}^{\text{cc}} N_n^{\text{sc}} + N_n^{\text{cc}} N_{n+1}^{\text{sc}} \\ &= \sum_{k=1}^n N_k^{\text{cc}} N_{k+1}^{\text{sc}}. \end{aligned} \quad (10)$$

Here, note that the complexity of CV-SD can be seen as a special case CSD; the CSD complexity with  $N_k^{\text{cc}} = L$  for  $\forall k$  becomes the CV-SD complexity. Note that the  $N_k^{\text{sc}}$  in (10) is identical to that in (9).

Now, we proceed to analyze the complexities of the CV-SD and CSD. We first analyze the complexity of CSD. Then the complexity of CV-SD can be easily derived by using the results of CSD complexity.

#### B. CSD complexity and CV-SD complexity

The expected complexity of CSD over  $\mathbf{H}$ ,  $\bar{\mathbf{s}}$ , and  $\mathbf{v}$  is

$$\mathbb{E}[\mathcal{C}_{\text{CSD-C}}] = \sum_{k=1}^n \mathbb{E} \left[ N_k^{\text{cc}} N_{k+1}^{\text{sc}} \right]. \quad (11)$$

For simplicity of the derivation, we assume  $m=n$  in the sequel. But, it can be easily seen that the result for the general case  $m>n$  remains the same.

Since the complexity is averaged over  $\bar{\mathbf{s}}$  in this section ( $\bar{\mathbf{s}}$  is not fixed), we consider  $\tilde{\Delta}_k$  and  $d_k$  as functions of not only  $\mathbf{s}$  but also  $\bar{\mathbf{s}}$ . Now,  $E[N_k^{cc} N_{k+1}^{sc}]$  can be written as follows

$$\begin{aligned} & E[N_k^{cc} N_{k+1}^{sc}] \\ &= E \left[ \sum_{s_k} I\{\tilde{\Delta}_k(s_k, \bar{s}_k) \leq C\} \sum_{\mathbf{s}_{k+1:n}, \bar{\mathbf{s}}_{k+1:n}} I\{d_{k+1}(\mathbf{s}_{k+1:n}, \bar{\mathbf{s}}_{k+1:n}) \leq C\} \right] \\ &= \sum_{s_{k:n}} E \left[ I\{\tilde{\Delta}_k(s_k, \bar{s}_k) \leq C\} \cdot I\{d_{k+1}(\mathbf{s}_{k+1:n}, \bar{\mathbf{s}}_{k+1:n}) \leq C\} \right] \quad (12) \\ &= \sum_{s_{k:n}} \Pr(\tilde{\Delta}_k(s_k, \bar{s}_k) \leq C, d_{k+1}(\mathbf{s}_{k+1:n}, \bar{\mathbf{s}}_{k+1:n}) \leq C) \\ &\stackrel{(a)}{=} \frac{1}{L^{n-k+1}} \sum_{s_{k:n}} \sum_{\bar{s}_{k:n}} \Pr(\tilde{\Delta}_k(s_k, \bar{s}_k) \leq C, d_{k+1}(\mathbf{s}_{k+1:n}, \bar{\mathbf{s}}_{k+1:n}) \leq C), \end{aligned}$$

where  $I\{\cdot\}$  is the indicator function which is 1 for the condition inside the bracket is true, otherwise 0, and (a) is from  $\Pr(\bar{\mathbf{s}}_{k:n}) = 1/L^{n-k+1}$ .

Before we move on further, we introduce a definition and a lemma which are useful for further simplification of (12).

*Definition 2: (non-negative correlation)* Two random events  $\mathcal{A}$  and  $\mathcal{B}$  are said to be *non-negatively correlated* if  $\text{cov}(I\{\mathcal{A}\}, I\{\mathcal{B}\}) \geq 0$ . We use the tilde symbol  $\sim$  between two events, i.e.,  $\mathcal{A} \sim \mathcal{B}$ , to imply that the two are *non-negatively correlated*.

*Lemma 3:*  $\mathcal{A} \sim \mathcal{B}$  if and only if  $\Pr(\mathcal{A}\mathcal{B}) \geq \Pr(\mathcal{A})\Pr(\mathcal{B})$ .

*Proof:*  $\text{cov}(I\{\mathcal{A}\}, I\{\mathcal{B}\})$  can be written as follows,

$$\begin{aligned} & \text{cov}(I\{\mathcal{A}\}, I\{\mathcal{B}\}) \\ &= E[(I\{\mathcal{A}\} - E[I\{\mathcal{A}\}]) (I\{\mathcal{B}\} - E[I\{\mathcal{B}\}])] \\ &= E[I\{\mathcal{A}\}I\{\mathcal{B}\}] - E[I\{\mathcal{A}\}]E[I\{\mathcal{B}\}] \\ &= \Pr(\mathcal{A}\mathcal{B}) - \Pr(\mathcal{A})\Pr(\mathcal{B}). \end{aligned}$$

Thus, for  $\text{cov}(I\{\mathcal{A}\}, I\{\mathcal{B}\}) \geq 0$ , it is definite that  $\Pr(\mathcal{A}\mathcal{B}) \geq \Pr(\mathcal{A})\Pr(\mathcal{B})$ , or vice-versa.  $\square$

Here we aim to show  $I\{d_{k+1}(\mathbf{s}_{k+1:n}, \bar{\mathbf{s}}_{k+1:n}) \leq C\} \sim I\{\tilde{\Delta}_k(s_k, \bar{s}_k) \leq C\}$ . To this end, we first show  $I\{d_{k+1} \leq C\} \sim I\{d_1 \leq C\}$ , and then  $I\{d_1 \leq C\} \sim I\{\tilde{\Delta}_k \leq C\}$ , and thus  $I\{d_{k+1} \leq C\} \sim I\{\tilde{\Delta}_k \leq C\}$ . Before we move on, note the inequalities  $d_{k+1} \leq d_1$  and  $\tilde{\Delta}_k \leq d_1$  from (3) and (6). Now, we show that  $I\{d_{k+1} \leq C\} \sim I\{d_1 \leq C\}$  by showing the following,  $\Pr(d_{k+1} \leq C, d_1 \leq C) = \Pr(d_1 \leq C) \geq \Pr(d_{k+1} \leq C)\Pr(d_1 \leq C)$ . Thus, the first is shown. Now, for the second, we show that  $\Pr(d_1 \leq C, \tilde{\Delta}_k \leq C) = \Pr(d_1 \leq C) \geq \Pr(d_1 \leq C)\Pr(\tilde{\Delta}_k \leq C)$ , thus  $I\{d_1 \leq C\} \sim I\{\tilde{\Delta}_k \leq C\}$ . Therefore,  $I\{d_{k+1}(\mathbf{s}_{k+1:n}, \bar{\mathbf{s}}_{k+1:n}) \leq C\} \sim I\{\tilde{\Delta}_k(s_k, \bar{s}_k) \leq C\}$ .

Now, return to the discussion of (12). Let  $\mathcal{A} := \{\tilde{\Delta}_k(s_k, \bar{s}_k) \leq C\}$  and  $\mathcal{B} := \{d_{k+1}(\mathbf{s}_{k+1:n}, \bar{\mathbf{s}}_{k+1:n}) \leq C\}$ . Using Lemma 3, the joint probability  $\Pr(\tilde{\Delta}_k(s_k, \bar{s}_k) \leq C, d_{k+1}(\mathbf{s}_{k+1:n}, \bar{\mathbf{s}}_{k+1:n}) \leq C)$  in (12) is lower bounded by  $\Pr(\tilde{\Delta}_k(s_k, \bar{s}_k) \leq C)\Pr(d_{k+1}(\mathbf{s}_{k+1:n}, \bar{\mathbf{s}}_{k+1:n}) \leq C)$ . Therefore, (12) becomes

$$\begin{aligned} & E[N_k^{cc} N_{k+1}^{sc}] \geq \\ & \frac{1}{L^{n-k+1}} \sum_{s_{k:n}} \sum_{\bar{s}_{k:n}} \Pr(\tilde{\Delta}_k(s_k, \bar{s}_k) \leq C) \Pr(d_{k+1}(\mathbf{s}_{k+1:n}, \bar{\mathbf{s}}_{k+1:n}) \leq C). \end{aligned}$$

We compute  $\Pr(\tilde{\Delta}_k(s_k, \bar{s}_k) \leq C)$  first, and then  $\Pr(d_{k+1}(\mathbf{s}_{k+1:n}, \bar{\mathbf{s}}_{k+1:n}) \leq C)$ . Before we proceed, we note the following lemma which will be useful for our analysis.

*Lemma 4:* The elements of  $\mathbf{R}^{-1}$  are statistically independent to the elements of  $\tilde{\mathbf{v}}$ , if the elements of  $\mathbf{R}$  and  $\tilde{\mathbf{v}}$  are independent.

*Proof:* Let  $f(\mathbf{R})$  a function of  $\mathbf{R}$ .  $f(\mathbf{R})$  and  $\tilde{\mathbf{v}}$  are independent as  $\mathbf{R}$  and  $\tilde{\mathbf{v}}$  are independent. Let  $f(\mathbf{R}) = \mathbf{R}^{-1}$ ;  $\mathbf{R}^{-1}$  is a function of  $\mathbf{R}$  as it determined by the determinant of  $\mathbf{R}$  and the cofactors of  $\mathbf{R}$ .  $\square$

*Lemma 5:* The probability  $\Pr(\tilde{\Delta}_k(s_k, \bar{s}_k) \leq C)$  is lower bounded by

$$\Pr(\tilde{\Delta}_k(s_k, \bar{s}_k) \leq C) \geq \max \left\{ 0, 1 - \frac{1}{C} \left( \left| \bar{s}_k - s_k \right|^2 \cdot n + \sigma_v^2 \right) \right\}. \quad (13)$$

*Proof:* See Appendix A.  $\square$

Now, we compute a lower bound on  $\Pr(d_{k+1}(\mathbf{s}_{k+1:n}, \bar{\mathbf{s}}_{k+1:n}) \leq C)$ .

*Lemma 6:* The probability  $\Pr(d_{k+1}(\mathbf{s}_{k+1:n}, \bar{\mathbf{s}}_{k+1:n}) \leq C)$  is lower bounded by

$$\begin{aligned} & \Pr(d_{k+1}(\mathbf{s}_{k+1:n}, \bar{\mathbf{s}}_{k+1:n}) \leq C) \\ & \geq \max \left\{ 0, 1 - \frac{1}{C} \left( \left\| \bar{\mathbf{s}}_{k+1:n} - \mathbf{s}_{k+1:n} \right\|^2 \cdot n + (n-k)\sigma_v^2 \right) \right\}. \quad (14) \end{aligned}$$

*Proof:* See Appendix B.  $\square$

Finally, we obtain the lower bound on the expected complexity of CSD.

*Theorem 7:* The expected complexity  $E[\mathcal{C}_{\text{CSD-C}}]$  is lower bounded by

$$E[\mathcal{C}_{\text{CSD-C}}] \geq \sum_{k=1}^n L^{n-k+1} \cdot \max\{0, 1 - \beta\} \cdot \max\{0, 1 - (n-k)\beta\}, \quad (15)$$

where

$$\beta := \frac{1}{C} \left( E \left[ \left| \bar{s}_k - s_k \right|^2 \right] \cdot n + \sigma_v^2 \right) \quad (16)$$

is the system scaling factor which is determined by the application and the algorithm parameters. The detailed explanation on this is given in the following subsection.

*Proof:* See Appendix C.  $\square$

The expected complexity for the CV-SD can be easily

obtained by using similar procedure, but only with (9) and Lemma 6.

*Theorem 8:* The expected complexity  $E[\mathcal{C}_{\text{SD-C}}]$  is lower bounded by

$$E[\mathcal{C}_{\text{SD-C}}] \geq \sum_{k=1}^n L^{n-k+1} \cdot \max\{0, 1 - (n-k)\beta\}. \quad (17)$$

### C. Complexity reduction behavior of CV-SD and CSD

In this subsection, it is seen that the CSD complexity can be written as the product of the CV-SD complexity and the additional complexity reduction factor in CSD to the CV-SD; refer to (22). We first evaluate the CV-SD complexity behavior and then explain the additional complexity reduction factor in CSD later on. For easy evaluation of the complexity behavior, the max functions in (15) and (17) are ignored.

The CV-SD complexity,  $E[\mathcal{C}_{\text{SD-C}}]$ , without the max function becomes

$$E[\mathcal{C}_{\text{SD-C}}] \geq \sum_{k=1}^n L^{n-k+1} (1 - \eta_k^{\text{SD-C}}), \quad (18)$$

where

$$\eta_k^{\text{SD-C}} := (n-k)\beta. \quad (19)$$

Here,  $L^{n-k+1}$  is the total number of nodes at the  $k^{\text{th}}$  level of the tree. Among the nodes,  $\eta_k^{\text{SD-C}}$  portion of them are excluded from PED computations. This gives the complexity reduction relative to the straight-forward ML implementation. This portion increases as the level of the tree,  $k$ , decreases. This is because the chance of pruning by SC increases for lower levels of the tree for PED accumulates as the level decreases. This is common in general for all SDs.

Now let us evaluate the behavior of  $E[\mathcal{C}_{\text{SD-C}}]$  for parameters of the systems or the algorithm. The portion  $\eta_k^{\text{SD-C}}$  is proportional to  $\beta$ . Use the definition of SNR

$$\text{SNR} = \frac{E[\|\mathbf{H}\mathbf{s}\|^2]}{E[\|\mathbf{n}\|^2]} = \frac{m}{\sigma_v^2}, \quad (20)$$

and get the insight on the complexity behavior related to SNR. Since  $\eta_k^{\text{SD-C}} \propto \beta$ , the behavior of  $\beta$  explains the complexity reduction behavior in the CV-SD. By applying SNR, it is expressed as

$$\beta = \frac{\sigma_v^2}{C} \left( E\left[|\bar{s}_i - s_i|^2\right] \text{SNR} + 1 \right). \quad (21)$$

It is seen that the complexity reduces as SNR increases. Here, we also see  $\beta$  is a decreasing function of the sphere radius  $C$ . Hence, it would be better off to employ a smaller  $C$  which still contains a solution inside the sphere.  $\beta$  is proportional also to average intra-constellation squared distance  $E\left[|\bar{s}_i - s_i|^2\right]$ . Here

note that  $E\left[|\bar{s}_i - s_i|^2\right]$  is not determined by users. It is given when the application is determined; for example, it is 2 for QAM, PSK, and (8,8) 16 star QAM cases, and 1.8163 for (8,24,32) 64 star QAM case (Section. VI).

We can see the complexity difference of the CV-SD to the RV-SD. Consider the complexity reduction factor of the RV-SD,  $\eta_k^{\text{SD-R}}$ , which can be easily obtained by using (8) and Lemma 6. It can be expressed as  $\eta_k^{\text{SD-R}} = (n-k+1)\beta$ . Here, we notice that the complexity reduction factor  $\eta_k^{\text{SD-C}}$  for the CV-SD has one less  $\beta$  than  $\eta_k^{\text{SD-R}}$  for the RV-SD. It is seen as expected from the inherent characteristic of the CV-SD, the  $L$ -expansion property. Actually, the direct comparison of  $\eta_k^{\text{SD-C}}$  and  $\eta_k^{\text{SD-R}}$  is not fair for the system model for RV-SD and hence  $\beta$  is different. But, at least, we can see the inefficiency of the CV-SD.

In the following, we study the complexity reduction behavior of CSD. We can see that the complexity reduction behavior of CSD is the same as that of the CV-SD except that there is additional complexity reduction term,  $\max\{0, (1-\beta)\}$ .

Therefore, here, we only evaluate the additional complexity reduction in CSD to the CV-SD. By additional complexity reduction, we mean the complexity reduction to the CV-SD, not to the straight-forward ML implementation. Ignoring the max function,  $E[\mathcal{C}_{\text{CSD-C}}]$  in (15) becomes

$$E[\mathcal{C}_{\text{CSD-C}}] \geq \sum_{k=1}^n L^{n-k+1} (1 - \eta_k^{\text{SD-C}}) (1 - \zeta^{\text{CSD-C}}), \quad (22)$$

where

$$\zeta^{\text{CSD-C}} := \beta \quad (23)$$

is additional complexity reduction factor in CSD compared to the CV-SD. As  $\beta$  is not a function of  $k$ , it can be directly written as

$$E[\mathcal{C}_{\text{CSD-C}}] = (1 - \zeta^{\text{CSD-C}}) \cdot E[\mathcal{C}_{\text{SD-C}}] = (1 - \beta) \cdot E[\mathcal{C}_{\text{SD-C}}]. \quad (24)$$

The lower bounds are ignored for the simplicity. Therefore, additional complexity reduction factor of CSD to the CV-SD becomes  $\zeta^{\text{CSD-C}} = \beta$  itself.

Here, we can see that the lower bound on  $E[\mathcal{C}_{\text{CSD-C}}]$  is always smaller than or equal to that on  $E[\mathcal{C}_{\text{SD-C}}]$  for all the scenarios since  $\zeta_k^{\text{CSD-C}} = \beta$  is nonnegative. Therefore, CSD is expected to outperform the CV-SD in any system settings (Section. VI); actually, this can be also seen in (10) for  $N_k^{\text{cc}} \leq L$ . This makes CSD more suited to complex valued systems than the CV-SD in terms of complexity.

Since  $\zeta_k^{\text{CSD-C}} = \beta$ ,  $\zeta_k^{\text{CSD-C}}$  can be evaluated solely by analyzing (21). As it is seen in (21), the additional reduction becomes more significant as SNR increases. This means that CSD is a powerful tool for complexity reduction in high SNR regimes since not only the complexity reduction relative to the

straight-forward ML implementation, but also the additional complexity reduction to the CV-SD becomes significant. It is seen in the simulations that in SNR regions for the SER around  $10^{-2}$  the additional complexity reduction to the CV-SD is substantial.

#### D. Complexity for the real valued version of CSD

There is a remark for the utilization of the complexity analysis of CSD in this section on the real valued systems. Sweatman and Thompson propose an SD-like algorithm for the real valued systems with additional simple test [22]; the test has a form similar to ours. But, they do not provide the complexity analysis. Even though their derivation for the test hence the test itself is different from ours, our complexity analysis can be used for their algorithm. It can be done just by replacing complex valued matrices and vectors in (7) with real valued ones. Note that our test in this paper is  $\Delta_k(s_k) = \Re^2(x_k - s_k) + \Im^2(x_k - s_k) \leq C \cdot \delta_k^2$ , while the one in [22] is  $\Re^2(x_k - s_k) \leq C \cdot \delta_k^2$  and  $\Im^2(x_k - s_k) \leq C \cdot \delta_k^2$ . The test in this paper is tighter than that in [22] as  $\max\{\Re^2(x_k - s_k), \Im^2(x_k - s_k)\} \leq \Re^2(x_k - s_k) + \Im^2(x_k - s_k) \leq C \cdot \delta_k^2$ . This means that the test in this paper may bring more pruning which is through simple tests. Note also that we derive (7) with Cauchy-Schwarz inequality directly from the SC while [22] uses Lagrange multipliers method in addition to the manipulation of the SC via complex singular value decomposition (SVD) of the channel matrix. We think that the derivation of CC in this paper is even simpler and hence clearer than that of [22]. In addition, readers can have better insight on the relationship between the proposed constraint and the original SC in this paper. Here, note that the primary purpose of CSD is on the flexibility on the choice of 2D constellations, not rectangular QAM only constellations for real valued systems. The real valued version of the CSD, and also the one in [22] are useful only when explicit PED computations are required for SC tests in real valued systems for some reasons.

## VI. SIMULATION RESULTS

### A. Simulation Setup

In this section, we show the complexity reduction capability of the proposed CSD using system simulations. We compare the proposed CSD with the baseline CV-SD which is also directly applicable to general complex valued constellations. To show the effectiveness of the proposed CSD in general 2D constellations, we consider star QAM, rectangular QAM, and PSK constellations in simulations. Here, note that the usage of CSD is not limited to these three constellations; it is applicable to arbitrary complex valued constellations. We use  $4 \times 4$  and  $6 \times 6$  MIMO systems with (8, 8) star 16 QAM for the ring ratio of 2, (4, 24, 32) star 64 QAM for the ring ratios of (2, 3) [7],<sup>4</sup> rectangular 16 QAM, rectangular 64 QAM, 8 PSK, and 32 PSK.

<sup>4</sup> The ring ratios indicates the ratios of the minimum ring amplitude to the other ring amplitude.

The proposed CSD and the CV-SD employs depth-first tree search. The initial radius is set to  $C_0 = \alpha n \sigma^2$  where  $\alpha$  is determined so that a solution is found with a high probability,  $1 - \varepsilon = 0.99$ , in the sphere [18]. If no solution found, the radius is increased until a solution is found [18]. During the tree search, the radius is updated whenever a candidate is found to be in the sphere radius. We employ the average number of PED computations as a metric for complexity. The number of PED computations is averaged over  $10^5$  runs of channels in each SNR value. The range of SNR is determined so that the symbol error rate (SER) of order of  $10^{-1}$ ,  $10^{-3}$ , and between them are obtained.

### B. Simulations

We first consider star QAM constellations. The usage of star QAM constellation is desirable in the applications which require low PAPR, compared to rectangular QAM constellations [7]. Fig. 2 plots the average numbers of PED computations for the CV-SD and the proposed CSD in  $4 \times 4$  MIMO systems with (8,8) star 16 QAM and in  $6 \times 6$  MIMO systems with (8,24,32) star 64 QAM. The proposed CSD reduces the complexity of the CV-SD considerably. We observe that CSD outperforms the CV-SD by 49%, 54%, 62%, 69% at SNR (dB) of 17, 19, 21, 23 in  $4 \times 4$  MIMO systems for (8,8) star 16 QAM. For  $6 \times 6$  MIMO systems with (8,24,32) star 64 QAM, CSD reduces the complexity of the CV-SD by 59%, 64%, 69%, 75% at SNR (dB) of 24, 26, 28, 30. As discussed in Section V-B, the complexity reduction factor increases as SNR increases; see the dashed lines in Fig. 2. Here, note that this significant complexity reduction in CSD is obtained without compromising its ML performance (Fig. 2).

We also consider rectangular QAM and PSK constellations. It is also observed that CSD performs better than the CV-SD by large margins in these constellations. For rectangular QAM constellations, CSD outperforms the CV-SD by 48%, 54%, 61%, 69% at SNR (dB) of 17, 19, 21, 23 in  $4 \times 4$  systems with 16 QAM (Fig. 3 (a)), and 59%, 63%, 67%, 74% at SNR (dB) of 24, 26, 28, 30 in  $6 \times 6$  systems for 64 QAM (Fig. 3 (b)), respectively.

For PSK constellations, the respective complexity reduction ratings of CSD from the CV-SD are 37%, 49%, 62%, 72% at SNR (dB) of 14, 17, 20, 23 in  $4 \times 4$  systems with 8 PSK (Fig. 4 (a)), and 70%, 75%, 79%, 83% at SNR (dB) of 26, 28, 30, 32 in  $6 \times 6$  systems with 32 PSK (Fig. 4 (b)).

The patterns of the complexity reduction of CSD in rectangular QAM and PSK constellations are similar to that of in star QAM constellations. The complexity reduction is considerable in all the SNR regions considered in the experiment. The complexity reduction gain is particularly large in higher SNR region.

### C. Special complexity reduction behavior in CSD

We note that there is significant complexity reduction of CSD compared to the CV-SD particularly in high SNR regions. Moreover, the complexity reduction factor gets larger as the

SNR increases. It is a unique complexity reduction behavior of CSD which utilizes additional constraint in complex valued systems. In single constraint based SD, not only the constraint of a lower complexity algorithm but also that of the reference algorithm usually becomes efficient in high SNR region. If the asymptotic efficiencies of both constraints are the same, the complexities of both tend to converge [10], [11], [15], [20]. Actually, at the extremely high SNR, the average complexities of them become almost the same as only one node per level survives from the constraint test (SC test) with high probability, thereby only one PED computation is required for a level of the tree.

In CSD, CC tests reduce the complexity of the search additionally. This gives the complexity reduction to the CV-SD. The improved efficiency of the CC in high SNR directly applies to the additional complexity reduction capability of CSD to the CV-SD. That is why additional complexity reduction in CSD to the CV-SD becomes more as SNR increases, rather than becoming smaller; refer to (23) and (21). It is also true even at an extremely high SNR. At a glance, it seems that the complexities of the two algorithms become almost the same in the region as both the constraint tests become strict, thereby only one node per level survives in the constraint tests. But, it is not true. Even if only one node per level survives in SC tests,  $N_k^{sc} = 1$ ,  $L$  PED computations need to be done for each level of the tree in the CV-SD because of the  $L$ -expansion property; refer to (9). Therefore, it still needs more than one PED computations per level in the CV-SD. However, even though

CSD is a CV-SD, it can achieve one PED computation per level. It is because the CC tests become so strict in extremely high SNR region that only one constellation point for each element of the vector  $\mathbf{s}$  passes the test with high probability; this can be seen in (10) by letting  $N_k^{cc} = 1$  and  $N_k^{sc} = 1$ . This makes it possible to have larger additional complexity reduction in higher SNR regions.

#### D. Remarks on the theoretical lower bound

Note that we do not include the comparison to the theoretical bound in this section. Remember that the objective of the theoretical analysis (Section V) is to evaluate the pattern of the complexity of the CV-SD and that of CSD. This objective is common to most of SD complexity analysis [15], [19]-[21]. The theoretical analysis of SD which is tight to the experiment results is not available. It is because *i*) the radius updates (Table I – Step 7) which affect the complexity is not easy to be tracked down precisely in the analysis. For example, it requires the calculation of the distribution of the radii to be updated; it appears to be a formidable task [17]. *ii*) The radius increase (Table I – Step 8) is not captured in the complexity analysis for analytical tractability. In addition, several lower bounds on the expected complexity are taken in the analysis aiming to have a simple form in the final result. That is why we do not include the comparison to the theoretical bound. However, please note that the pattern of the additional complexity reduction of CSD to the CV-SD follows the analyzed theoretical behavior in Section V (Section VI-B and VI-C).

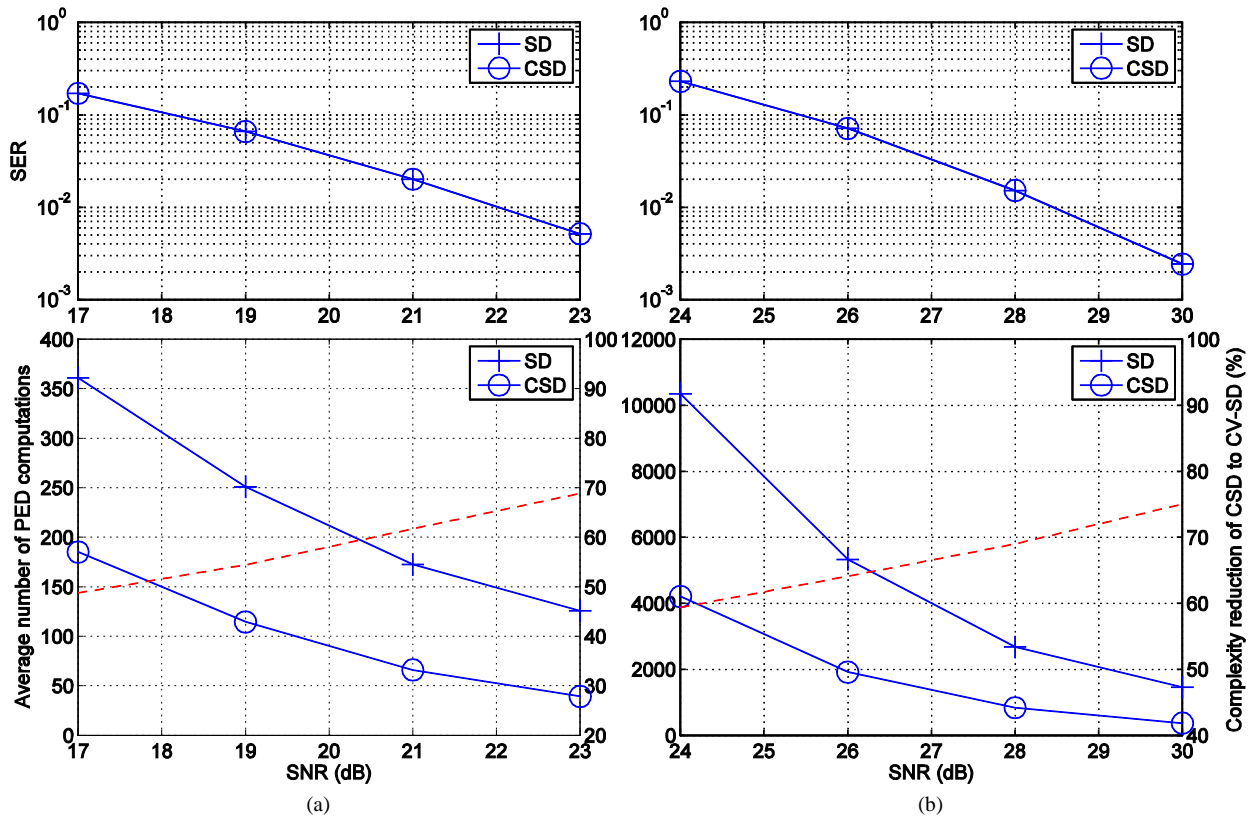


Fig. 2. SER performance and complexity of the CV-SD and the proposed CSD for 4x4 MIMO systems with (8,8) star 16 QAM and 6x6 MIMO systems with (8,24,32) star 64 QAM.

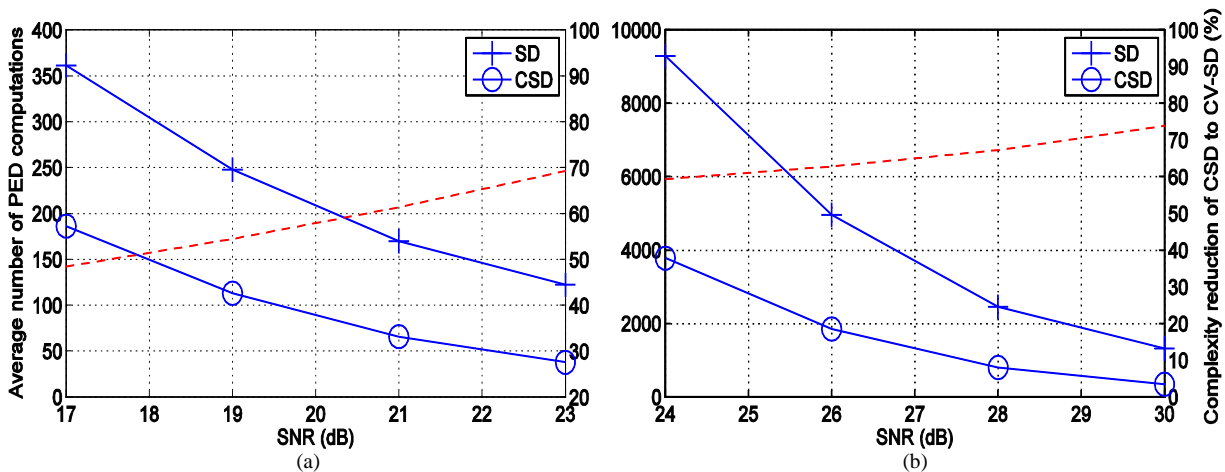


Fig. 3. Complexity of the CV-SD and the proposed CSD for (a) 4×4 MIMO systems with rectangular 16 QAM and (b) 6×6 MIMO systems with rectangular 64 QAM.

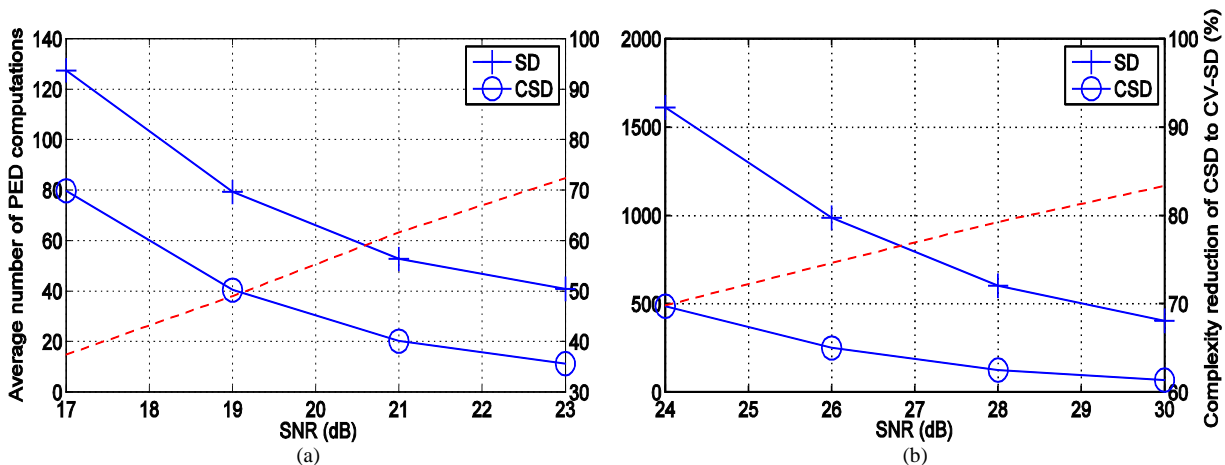


Fig. 4. Complexity of the CV-SD and the proposed CSD for (a) 4×4 MIMO systems with 8 PSK and (b) 6×6 MIMO systems with 32 PSK.

## VII. CONCLUSION

In this paper, we have proposed CSD, a low complexity CV-SD, for general 2D constellations. CSD aims at reducing the number of explicit PED computations, the most complex operations in SD. It uses the circular constraint (CC) for prescreening candidates and pruning some of them even before executing the PED computations. It gives a large reduction in the number of PED computations. This is shown in analysis and also in simulation. As a result, the proposed CSD becomes surely a good candidate for a general 2D constellation low complexity MIMO detector. Now with the proposed CSD, it becomes possible to decode signals with integer data rate (not only for  $m=2^i$ ,  $i=1,2,\dots$ ) and arbitrary shape of 2D constellations which may be optimal for target applications with low complexity while achieving the ML performance as CSD is compatible to general 2D constellation. Many 2D constellations can be handled in this single CSD algorithm without any additional constellation-dependent functionality.

## APPENDIX A

### PROOF OF LEMMA 5

$E[\tilde{\Delta}_k(s_k, \bar{s}_k)]$  is expressed as follows

$$\begin{aligned} E[\tilde{\Delta}_k(s_k, \bar{s}_k)] &= E\left[\frac{|\bar{s}_k - s_k + \mathbf{R}_{k,-}^{-1} \tilde{\mathbf{v}}|^2}{\|\mathbf{R}_{k,-}^{-1}\|^2}\right] \\ &= \frac{|\bar{s}_k - s_k|^2}{E[\|\mathbf{R}_{k,-}^{-1}\|^2]} + E\left[\frac{\left|\sum_{i=1}^n R_{k,j}^{-1} \cdot \tilde{v}_i\right|^2}{\|\mathbf{R}_{k,-}^{-1}\|^2}\right] \\ &\quad + 2(\bar{s}_k - s_k)^* E\left[\frac{\sum_{i=1}^n R_{k,j}^{-1} \cdot \tilde{v}_i}{\|\mathbf{R}_{k,-}^{-1}\|^2}\right], \end{aligned}$$

where  $R_{k,j}^{-1}$  is the  $(k, j)$  element of  $\mathbf{R}^{-1}$ .

The first term is upper bounded as follows,

$$\begin{aligned} \frac{|\bar{s}_k - s_k|^2}{\mathbb{E}\left[\|\mathbf{R}_{k,-}^{-1}\|^2\right]} &\stackrel{(a)}{\leq} |\bar{s}_k - s_k|^2 \mathbb{E}\left[\|\mathbf{R}_{-k}\|^2\right] \\ &\stackrel{(b)}{=} |\bar{s}_k - s_k|^2 \cdot n, \end{aligned}$$

where (a) is from  $\mathbb{E}\|\mathbf{R}_{k,-}^{-1}\|^2 \mathbb{E}\|\mathbf{R}_{-k}\|^2 \geq \mathbb{E}|\mathbf{R}_{k,-}^{-1} \mathbf{R}_{-k}| = 1$ , the Cauchy-Schwarz inequality, and (b) is from  $\|\mathbf{R}_{-k}\|^2 = \|\mathbf{Q}^* \mathbf{H}_{-k}\|^2 = \|\mathbf{H}_{-k}\|^2$ .

The second term becomes  $\sigma_v^2$  as follows,

$$\begin{aligned} &\mathbb{E}\left[\frac{\left|\sum_{i=1}^n R_{k,i}^{-1} \cdot \tilde{v}_i\right|^2}{\|\mathbf{R}_{k,-}^{-1}\|^2}\right] \\ &= \sum_{i=1}^n \mathbb{E}\left[\frac{|R_{k,i}^{-1} \cdot \tilde{v}_i|^2}{\|\mathbf{R}_{k,-}^{-1}\|^2}\right] + \sum_{i=1, j=1, i \neq j}^n \mathbb{E}\left[\frac{(R_{k,i}^{-1} \cdot \tilde{v}_i)^* (R_{k,j}^{-1} \cdot \tilde{v}_j)}{\|\mathbf{R}_{k,-}^{-1}\|^2}\right] \\ &\stackrel{(c)}{=} \sum_{i=1}^n \mathbb{E}\left[\frac{|R_{k,i}^{-1}|^2}{\|\mathbf{R}_{k,-}^{-1}\|^2}\right] \mathbb{E}[\tilde{v}_i^2] + \sum_{i=1, j=1, i \neq j}^n \mathbb{E}\left[\frac{R_{k,i}^{-1} R_{k,j}^{-1}}{\|\mathbf{R}_{k,-}^{-1}\|^2}\right] \mathbb{E}[\tilde{v}_i^*] \mathbb{E}[\tilde{v}_j] \\ &= \sigma_v^2, \end{aligned}$$

where (c) is from the independence of  $\tilde{\mathbf{v}}$  and  $\mathbf{R}^{-1}$  (Lemma 4).

The third term becomes zero as follows

$$\mathbb{E}\left[\frac{\sum_{i=1}^n R_{k,i}^{-1} \cdot \tilde{v}_i}{\|\mathbf{R}_{k,-}^{-1}\|^2}\right] = \sum_{i=1}^n \mathbb{E}\left[\frac{R_{k,i}^{-1}}{\|\mathbf{R}_{k,-}^{-1}\|^2} \tilde{v}_i\right] \stackrel{(d)}{=} \sum_{i=1}^n \mathbb{E}\left[\frac{R_{k,i}^{-1}}{\|\mathbf{R}_{k,-}^{-1}\|^2}\right] \mathbb{E}[\tilde{v}_i] = 0,$$

where (d) is also from the independence of  $\tilde{\mathbf{v}}$  and  $\mathbf{R}^{-1}$ .

Therefore,  $\mathbb{E}[\tilde{\Delta}_k(s_k, \bar{s}_k)] \leq |\bar{s}_k - s_k|^2 \cdot n + \sigma_v^2$ .

Now,  $\Pr(\tilde{\Delta}_k(s_k, \bar{s}_k) \leq C)$  is lower bounded by as follows,

$$\begin{aligned} \Pr(\tilde{\Delta}_k(s_k, \bar{s}_k) \leq C) &\stackrel{(a)}{\geq} \max\left\{0, 1 - \frac{1}{C} \mathbb{E}[\tilde{\Delta}_k(s_k, \bar{s}_k)]\right\} \\ &\geq \max\left\{0, 1 - \frac{1}{C} \left(|\bar{s}_k - s_k|^2 \cdot n + \sigma_v^2\right)\right\}, \end{aligned}$$

where (a) is from the Markov inequality and the max function is to make sure the probability to be nonnegative.

#### APPENDIX B PROOF OF LEMMA 6

$\mathbb{E}[d_{k+1}(\mathbf{s}_{k+1:n}, \bar{\mathbf{s}}_{k+1:n})]$  is expressed as follows

$$\begin{aligned} &\mathbb{E}\left[d_{k+1}(\mathbf{s}_{k+1:n}, \bar{\mathbf{s}}_{k+1:n})\right] \\ &= \sum_{i=k+1}^n \mathbb{E}\left[\left|\mathbf{R}_{i,i:n}(\bar{\mathbf{s}}_{i:n} - \mathbf{s}_{i:n}) + \tilde{v}_i\right|^2\right] \\ &= \sum_{i=k+1}^n \mathbb{E}\left[\left|\sum_{j=i}^n R_{i,j}(\bar{s}_j - s_j) + \tilde{v}_i\right|^2\right] \\ &\stackrel{(a)}{=} \sum_{i=k+1}^n \mathbb{E}\left[\left|\sum_{j=i}^n R_{i,j}(\bar{s}_j - s_j)\right|^2\right] + \sum_{i=k+1}^n \mathbb{E}\left[|\tilde{v}_i|^2\right] \\ &\stackrel{(b)}{=} \sum_{i=k+1}^n \left(\sum_{j=i}^n |\bar{s}_j - s_j|^2 \mathbb{E}\left[|R_{i,j}|^2\right]\right) \\ &\quad + \sum_{j=i, l=i, j \neq l}^n (\bar{s}_j - s_j)^* (\bar{s}_l - s_l) \mathbb{E}\left[R_{i,j}^*\right] \mathbb{E}\left[R_{i,l}\right] + (n-k)\sigma_v^2 \\ &\stackrel{(c)}{=} \sum_{i=k+1}^n \sum_{j=i}^n |\bar{s}_j - s_j|^2 \mathbb{E}\left[|R_{i,j}|^2\right] + (n-k)\sigma_v^2 \\ &= \sum_{j=k+1}^n |\bar{s}_j - s_j|^2 \sum_{i=k+1}^j \mathbb{E}\left[|R_{i,j}|^2\right] + (n-k)\sigma_v^2 \\ &\leq \sum_{j=k+1}^n |\bar{s}_j - s_j|^2 \mathbb{E}\left[\|\mathbf{R}_{-j}\|^2\right] + (n-k)\sigma_v^2 \\ &\stackrel{(d)}{=} \|\bar{\mathbf{s}}_{k+1:n} - \mathbf{s}_{k+1:n}\|^2 \cdot n + (n-k)\sigma_v^2, \end{aligned}$$

where (a) is from the independence of  $\tilde{\mathbf{v}}$  and  $\mathbf{R}$ , (b) is from the independence between the elements in  $\mathbf{R}$  [18], (c) is from the fact that any off-diagonal element of  $\mathbf{R}$  has mean zero [18], (d) is from  $\|\mathbf{R}_{-j}\|^2 = \|\mathbf{Q}^* \mathbf{H}_{-j}\|^2 = \|\mathbf{H}_{-j}\|^2$  and  $\|\bar{\mathbf{s}}_{k:n} - \mathbf{s}_{k:n}\|^2 = \sum_{j=k}^n |\bar{s}_j - s_j|^2$ .

Finally, using the Markov inequality,  $\Pr(d_{k+1}(\mathbf{s}_{k+1:n}, \bar{\mathbf{s}}_{k+1:n}) \leq C)$  is lower bounded by

$$\begin{aligned} &\Pr(d_{k+1}(\mathbf{s}_{k+1:n}, \bar{\mathbf{s}}_{k+1:n}) \leq C) \\ &\geq \max\left\{0, 1 - \frac{1}{C} \left(\|\bar{\mathbf{s}}_{k+1:n} - \mathbf{s}_{k+1:n}\|^2 \cdot n + (n-k)\sigma_v^2\right)\right\}. \end{aligned}$$

#### APPENDIX C PROOF OF THEOREM 7

Starting from (12),

$$\begin{aligned} &\mathbb{E}[N_k^{cc} N_{k+1}^{sc}] \\ &= (1/L^{n-k+1}) \sum_{\mathbf{s}_{k:n}} \sum_{\bar{\mathbf{s}}_{k:n}} \Pr(\tilde{\Delta}_k(s_k, \bar{s}_k) \leq C, d_{k+1}(\mathbf{s}_{k+1:n}, \bar{\mathbf{s}}_{k+1:n}) \leq C) \\ &\stackrel{(a)}{\geq} (1/L^{n-k+1}) \sum_{\mathbf{s}_{k:n}} \sum_{\bar{\mathbf{s}}_{k:n}} \Pr(\tilde{\Delta}_k(s_k, \bar{s}_k) \leq C) \Pr(d_{k+1}(\mathbf{s}_{k+1:n}, \bar{\mathbf{s}}_{k+1:n}) \leq C) \\ &\stackrel{(b)}{\geq} (1/L^{n-k+1}) \sum_{\mathbf{s}_k} \sum_{\bar{\mathbf{s}}_k} \max\left\{0, 1 - \frac{1}{C} \left(|\bar{s}_k - s_k|^2 \cdot n + \sigma_v^2\right)\right\} \\ &\quad \cdot \sum_{\mathbf{s}_{k+1:n}} \sum_{\bar{\mathbf{s}}_{k+1:n}} \max\left\{0, 1 - \frac{1}{C} \left(\|\bar{\mathbf{s}}_{k+1:n} - \mathbf{s}_{k+1:n}\|^2 \cdot n + (n-k)\sigma_v^2\right)\right\} \end{aligned}$$

$$\begin{aligned}
&\stackrel{(c)}{\geq} L^{n-k+1} \cdot \max \left\{ 0, \frac{1}{L^2} \sum_{s_k} \sum_{\bar{s}_k} 1 - \frac{1}{C} \left( \left| \bar{s}_k - s_k \right|^2 \cdot n + \sigma_v^2 \right) \right\} \\
&\cdot \max \left\{ 0, \frac{1}{L^{2(n-k)}} \sum_{\mathbf{s}_{k+1:n}} \sum_{\bar{\mathbf{s}}_{k+1:n}} 1 - \frac{1}{C} \left( \left\| \bar{\mathbf{s}}_{k+1:n} - \mathbf{s}_{k+1:n} \right\|^2 \cdot n + (n-k)\sigma_v^2 \right) \right\} \\
&= L^{n-k+1} \cdot \max \left\{ 0, 1 - \frac{1}{C} \left( \mathbb{E} \left[ \left| \bar{s}_k - s_k \right|^2 \right] \cdot n + \sigma_v^2 \right) \right\} \\
&\cdot \max \left\{ 0, 1 - \frac{1}{C} \left( \mathbb{E} \left[ \left\| \bar{\mathbf{s}}_{k+1:n} - \mathbf{s}_{k+1:n} \right\|^2 \right] \cdot n + (n-k)\sigma_v^2 \right) \right\} \\
&= L^{n-k+1} \cdot \max \{ 0, 1 - \beta \} \cdot \max \{ 0, 1 - (n-k)\beta \},
\end{aligned}$$

where (a) is from Lemma 3, (b) is from Lemma 5 and 6, (c) is from  $\max \left\{ \sum_k a_k, \sum_k b_k \right\} \leq \sum_k \max \{ a_k, b_k \}$ , and (d) is from

$$\begin{aligned}
\sum_{\bar{s}_k} \sum_{s_k} 1 &= L^2, \quad \mathbb{E} \left[ \left| \bar{s}_k - s_k \right|^2 \right] = \frac{1}{L^2} \sum_{s_k} \sum_{\bar{s}_k} \left| \bar{s}_k - s_k \right|^2, \quad \sum_{\bar{\mathbf{s}}_{k+1:n}} \sum_{\mathbf{s}_{k+1:n}} 1 \\
&= L^{2(n-k)}, \quad \text{and} \quad \mathbb{E} \left[ \left\| \bar{\mathbf{s}}_{k+1:n} - \mathbf{s}_{k+1:n} \right\|^2 \right] \\
&= \frac{1}{L^{2(n-k)}} \sum_{\bar{\mathbf{s}}_{k+1:n}} \sum_{\mathbf{s}_{k+1:n}} \left\| \bar{\mathbf{s}}_{k+1:n} - \mathbf{s}_{k+1:n} \right\|^2.
\end{aligned}$$

A lower bound of  $\mathbb{E}[C_{\text{CSD-C}}]$  is obtained by applying the lower bound of  $\mathbb{E}[N_k^{cc} N_{k+1}^{sc}]$  to (11).

## REFERENCES

- [1] U. Fincke and M. Pohst, "Improved methods for calculating vectors of short length in a lattice, including a complexity analysis," *Math. Computation*, vol. 44, no. 2, pp. 463–471, Apr. 1985.
- [2] E. Agrell, T. Eriksson, A. Vardy, and K. Zeger, "Closest point search in lattices," *IEEE Trans. on Inf. Theory*, vol. 48, no. 8, pp. 2201–2214, Aug. 2002.
- [3] E. Viterbo and J. Boutros, "A universal lattice code decoder for fading channels," *IEEE Trans. on Inf. Theory*, vol. 45, no. 5, pp. 1639–1642, July 1999.
- [4] M. O. Damen, H. El Gamal, and G. Caire, "On maximum-likelihood detection and the search for the closest lattice point," *IEEE Trans. on Inf. Theory*, vol. 49, no. 10, pp. 2389–2402, Oct. 2003.
- [5] D. Pham, K. R. Pattipati, P. K. Willett, and J. Luo, "An Improved Complex Sphere Decoder for V-BLAST Systems," *IEEE Signal Processing Letters*, vol. 11, no. 9, pp. 748–751, Sep. 2004.
- [6] R. S. Mozos, and M. J. F.-G. Garcia, "Efficient Complex Sphere Decoding for MC-CDMA Systems," *IEEE Trans. on Wireless Communications*, vol. 5, no. 11, pp. 2992–2996, Nov. 2006.
- [7] R. Kobayashi, T. Kawamura, N. Miki, and M. Sawahashi, "Throughput Comparisons of Star 32/64 QAM Schemes Based on Mutual Information Considering Cubic Metric," *International Conference on Wireless Communications and Signal Processing (WCSP)*, Nanjing, China, Nov. 2011.
- [8] G. D. Forney and G. Ungerboeck, "Modulation and Coding for Linear Gaussian Channels," *IEEE Trans. on Inf. Theory*, vol. 44, no. 6, pp. 2284–2415, Oct. 1998.
- [9] I. Nevat, G. W. Peters, and J. Yuan, "Detection of Gaussian Constellations in MIMO Systems Under Imperfect CSI," *IEEE Trans. on Communications*, vol. 58, no. 4, pp. 1151–1160, Apr. 2010.
- [10] A. Burg, M. Borgmann, C. Simon, M. Wenk, M. Zellweger and W. Fichtner, "Performance tradeoffs in the VLSI implementation of the sphere decoding algorithm," in *Proc. IEE 3G Mobile Communication Conf.*, London, U.K., Oct. 2004.
- [11] A. Burg, M. Borgmann, M. Wenk, M. Zellweger, W. Fichtner, and H. Bölcskei, "VLSI implementation of MIMO detection using the sphere decoding algorithm," *IEEE Journal of Solid-State Circuits*, vol. 40, no. 7, pp. 1566–1577, July 2005.
- [12] B. M. Hochwald and S. ten Brink, "Achieving near-capacity on a multiple-antenna channel," *IEEE Trans. on Communications*, vol. 51, no. 3, pp. 389–399, Mar. 2003.
- [13] L. G. Barbero and J. S. Thompson, "Fixing the Complexity of the Sphere Decoder for MIMO detection," *IEEE Trans. on Wireless Communications*, vol. 7, no. 6, pp. 2131–2142, June 2008.
- [14] R. Gowaikar and B. Hassibi, "Statistical Pruning for Near-Maximum Likelihood Decoding," *IEEE Trans. on Signal Processing*, vol. 55, no. 6, pp. 2661–2675, June 2007.
- [15] B. Shim and I. Kang, "Sphere decoding with a probabilistic tree pruning," *IEEE Trans. on Signal Processing*, vol. 56, no. 10, pp. 4867–4878, Oct. 2008.
- [16] J. Ahn, H.-N. Lee, and K. Kim, "A Near-ML Decoding with Improved Complexity over Wider Ranges of SNR and System Dimension in MIMO Systems," *IEEE Trans. on Wireless Communications*, vol. 11, no. 1, pp. 33–37, Jan. 2012.
- [17] H. Vikalo and B. Hassibi, "On the Sphere-Decoding Algorithm II. Generalizations, Second-Order Statistics, and Applications to Communications," *IEEE Trans. on Signal Processing*, vol. 53, no. 8, pp. 2819–2834, Aug. 2005.
- [18] B. Hassibi and H. Vikalo, "On the Sphere-Decoding Algorithm I. Expected Complexity," *IEEE Trans. on Signal Processing*, vol. 53, no. 8, pp. 2806–2818, Aug. 2005.
- [19] J. Jaldén and B. Ottersten, "On the complexity of Sphere Decoding in Digital Communications," *IEEE Trans. on Signal Processing*, vol. 53, no. 4, pp. 1474–1484, Apr. 2005.
- [20] D. Seethaler and H. Bölcskei, "Performance and Complexity Analysis of Infinity-Norm Sphere-Decoding," *IEEE Trans. on Inf. Theory*, vol. 56, no. 3, pp. 1085–1105, Mar. 2010.
- [21] D. Seethaler, J. Jaldén, C. Studer, and H. Bölcskei, "On the Complexity Distribution of Sphere Decoding," *IEEE Trans. on Inf. Theory*, vol. 57, no. 9, pp. 5754–5768, Sep. 2011.
- [22] C. Z. W. H. Sweatman and J. S. Thompson, "Orthotope sphere decoding and parallelotope decoding – reduced complexity optimum detection algorithms for MIMO channels," *Signal Processing*, vol. 86, no. 7, pp. 1518–1537, Jul. 2006.